Inorganic Chemistry

pubs.acs.org/IC Article

Comparative Structural Study of Metal-Mediated Base Pairs Formed outside and inside DNA Molecules

Alicia Dominguez-Martin, Simona Galli, José A. Dobado, Noelia Santamaría-Díaz, Antonio Pérez-Romero, and Miguel A. Galindo*

Cite This: https://dx.doi.org/10.1021/acs.inorgchem.0c01210 Read Online

ACCESS | Metrics & More | Article Recommendations | Supporting Information

ABSTRACT: The formation of copper(II)-mediated base pairs involving pyridine-2,6-dicarboxylate derivatives and canonical nucleosides has proven to be a smart approach to introduce copper(II) ions at specific locations of DNA duplexes. However, the structural characteristics of these metalized base pairs have not yet been revealed, and their effect on DNA structures is difficult to assess. Herein, for the first time, we report on the different structural details of copper-mediated base pairs formed by themselves and in DNA duplexes. The individual base pairs [Cu(mcheld)(*N3*-Cyt)(H_2O)]·3H_2O (**1Cu_Cyt**), [Cu(mcheld)(*N7*-Ade)(H_2O)$_2$]·2H_2O (**1Cu_Ade**), [Cu(mcheld)(*N7*-Gua)(H_2O)] (**1Cu_Gua**), and [Cu(mcheld)(*N1*-^{7C}Ade)(H_2O)]·H_2O (**1Cu_^{7C}Ade**) were obtained from the reaction of the metal complex [Cu(mcheld)(H_2O)$_2$] (**1Cu**) (mcheld = 4-methoxypyridine-2,6-dicarboxylic acid) with model nucleosides (Cyt = *N1*-methylcytosine, Ade = *N9*-ethyladenine, Gua = *N9*-propylguanine, ^{7C}Ade = *N9*-propyl-7-deazaadenine). The crystal structure of the five complexes was determined by means of single-crystal X-ray diffraction. Furthermore, the formation of the **1Cu_Cyt** and **1Cu_Gua** base pairs in the middle of DNA duplexes, duplex **DNA$_{15}$** (917 atoms) and **DNA$_{10}$** (649 atoms), respectively, was studied using highly demanding *ab initio* computational calculations. These theoretical studies aimed to validate, from a structural point of view, whether base pairs of the kind **1Cu_nucleosides** can be included in a DNA double helix and how this situation affects the double-helical structure. The results indicate that the **1Cu_Cyt** and **1Cu_Gua** base pairs can be formed in a DNA molecule without significant structural constraints. In addition, the double-helix DNA structure remains virtually unchanged when it contains these Cu(II)-mediated base pairs.

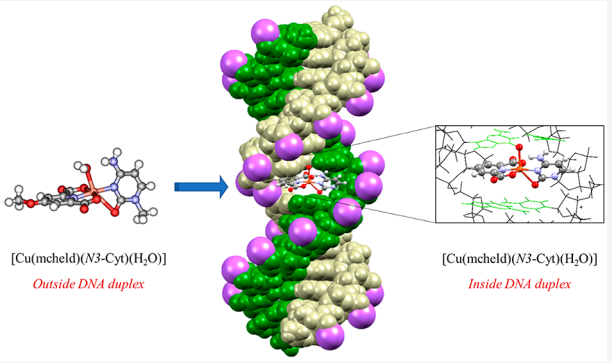

INTRODUCTION

The development of DNA-based nanotechnology has received deep attention due to the remarkable properties of nucleic acids.[1] DNA is very soluble in water, and its synthesis is well established, making it an ideal biopolymer for research purposes. The code programmability of DNA derives from the natural self-assembly capabilities of adenine−thymine (A-T) and guanine−cytosine (G-C) base pairs. The DNA structure and conformation can be rationally preprogrammed on the basis of the self-recognition abilities of DNA sequences,[2] leading to tailored structures that range from the nanometer to the micrometer scale.[3] In addition, the DNA genetic code can be further expanded if novel ligand-type nucleobases (LTNs), i.e. specific ligands replacing canonical nucleobases, are employed.[4] In this regard, different LTNs have been demonstrated to self-assemble inside DNA in the presence of metal ions, forming the so-called metal-mediated base pairs.[5] This strategy, first proposed by Shionoya's research group[6] and first achieved by Schultz,[4] has led to the formation of smart metal-mediated base pairs with different combinations, which include LTN-M-LTN and LTN-M-nucleobase pairs (M = metal ion).[7,8] Among the LTNs, some nucleobase analogues are capable of mimicking either Watson−Crick or Hoogsteen pairing in both the absence and presence of metal ions.[9−12] Remarkably, the use of LTNs has led to short oligonucleotides featuring specific transition-metal ions situated at precise locations inside a DNA double helix, with applications ranging from sensing to electron transport processes.[13−17] The formation of metal-mediated base pairs inside DNA is normally determined in solution using spectroscopic and spectrometric methodologies. However, unraveling the structural organization of these systems can be a complicated task due to the difficulty in either obtaining

Received: April 23, 2020

https://dx.doi.org/10.1021/acs.inorgchem.0c01210
Inorg. Chem. XXXX, XXX, XXX−XXX

crystals suitable for single-crystal X-ray diffraction, or performing structural high-resolution NMR studies. Notably, in some cases, solid-state crystallographic investigations and solution NMR studies have been carried out for DNA molecules containing metal-mediated base pairs.[18] Alternatively, theoretical computational procedures can help in revealing the structural aspects of metal-mediated base pairs. Such calculations are commonly performed for individual base pairs,[19,20] with few cases involving the DNA framework.[21,22]

The ligand pyridine-2,6-dicarboxylic acid (Cheld, a planar tridentate ligand) and its carboxyamide derivative[23] were among the pioneering ligands to be employed in the formation of metal-mediated base pairs. Cheld has been widely used in the preparation of metalated double-stranded DNA (ds-DNA) molecules via the formation of metal-mediated base pairs. Initially, Cheld and pyridine were employed to introduce Cu(II) ions into DNA duplexes by forming unsymmetrical [3 + 1] metal−base pairs. This approach led to the formation, in solution, of DNA duplexes containing Cheld-Cu-nucleobase mismatches, which showed higher thermal stability in comparison to the unmetalated counterparts.[4] The stabilization of these mismatches followed the trend adenine > cytosine > guanine, with no data for thymidine mismatches. These results demonstrated that the ligand Cheld can be employed to form metal-mediated base pairs with canonical bases within ds-DNA molecules.

The crystal structure of a DNA duplex containing one Cheld-Cu-pyridine metallo-base pair was determined,[24] as well as the crystal structure of the complex itself,[25,26] demonstrating the predictable coplanar arrangement between Cheld and pyridine in both cases. However, no further studies have been performed to fully reveal the structure and conformation of Cheld-Cu-nucleoside systems, where noncoplanar arrangements between the units can be anticipated. In this regard, it is important to compare the structure of metal-mediated base pairs when they are prepared inside and outside a double helix, in order to determine the effect of the DNA scaffold on the final arrangement. In this respect, Cheld-Cu-nucleoside systems are important representative examples.

To the best of our knowledge, only the crystal structure of the Cheld-Cu-adenine ternary complex[27] and the interaction of other iminodiacetic acid based copper(II) complexes toward adenine derivatives[28] have been reported. Though the molecular structure of Cheld-Cu-nucleoside systems could be foretold in principle on the basis of these previously described systems, detailed, experimentally derived structural information at the molecular and crystal-packing level is still needed to accurately understand the structural implications that the Cheld-Cu-nucleoside systems can have in DNA molecules.

Ultimately, determining the crystal and molecular structure of metal-mediated base pairs will provide fundamental information that can be used in the design of novel metal−DNA systems, potentially finding applications in different areas, from catalysis to charge transport.

In this context, we report herein the preparation and solid-state characterization of complexes of the type Cheld-Cu-nucleoside as well as, utilizing *ab initio* theoretical calculations, their organization inside DNA duplexes, in an effort to get some insight into the molecular arrangement of these systems when they are prepared by themselves and in the context of a DNA molecule.

EXPERIMENTAL SECTION

Materials and Methods. 1-Methylcytosine (Cyt),[29] *N*9-ethyladenine (Ade),[30] and diethyl-4-hydroxypyrimidine-2,6-carboxylic acid (decheld)[31] were synthesized according to literature procedures. 6-Amino-7-deazapurine, 6-chloro-2-amino-7-deazapurine, adenine, sodium hydride (60% oil dispersion), anhydrous *N*,*N*-dimethylformamide, 1-iodopropane, and the oligonucleotides d(Ade)$_{15}$, d(^{7C}Ade)$_{15}$, d(Cyt)$_{15}$ and d(Gua)$_{10}$ were purchased from Sigma-Aldrich. ^{1}H NMR spectra were recorded with a Bruker AMX instrument working at 300 MHz. ^{13}C NMR spectra were recorded with a Bruker Neo 500 MHz spectrometer. Elemental analyses were carried out with a Fisons-Carlo Erba Model EA 1108 analyzer. CD spectra were recorded on a JASCO J-815 spectrometer. High-resolution electrospray mass spectrometry was performed with a Waters LCT Premier XE mass spectrometer. Infrared (IR) spectra were registered with a Bruker Tensor-27 FT-IR spectrometer.

Synthesis of the Ligands. *Diethyl-4-methoxypyrimidine-2,6-dicarboxylic Acid (demcheld).* To a solution of decheld (3.00 g, 12.50 mmol) in anhydrous *N*,*N*-dimethylformamide (150 mL) was added sodium hydride (0.50 g, 12.50 mmol) under N_2. The reaction mixture was stirred for 30 min at room temperature. After this time, iodomethane (0.79 mL, 12.50 mmol) was added and the mixture was stirred under N_2 for 48 h. The solvent was then removed under reduced pressure, and the product was diluted in dichloromethane (150 mL) and washed with aqueous sodium hydrogen carbonate (10% m/m, 150 mL) and brine (150 mL). The organic layers were collected, dried over magnesium sulfate, filtered off, and concentrated in vacuo, giving the title compound as a white powder (3.00 g, 94% yield). ^{1}H NMR (300 MHz, DMSO-d_6): δ (ppm) 7.72 (s, 2H; *CH*), 4.38 (q, J = 7.1 Hz, 4H; CH_2), 3.98 (s, 3H; CH_3), 1.34 (t, J = 7.1 Hz, 6H; CH_3). HRMS (ESI): m/z calcd for $C_{12}H_{16}NO_5$ $[M + H]^+$, 254.1028; found, 254.1037.

4-Methoxypyridine-2,6-dicarboxylic Acid (mcheld). demcheld (2.00 g, 8.37 mmol) was dissolved in 0.5 M aqueous sodium hydroxide (25 mL), and the solution thus obtained was refluxed overnight. Then, the solution was acidified with concentrated hydrochloric acid until the pH reached 3.6 and was concentrated under reduced pressure to give the title compound as a white precipitate, which was filtered off and dried under vacuum (1.21 g, 58% yield). ^{1}H NMR (300 MHz, DMSO-d_6): δ (ppm) 7.36 (s, 2H; *CH*), 3.80 (s, 3H; CH_3). IR (ν/cm^{-1}): 3564.7, 3429.8, 3084.3, 2923, 1722, 1631.5, 1601, 1574.7, 1465.8, 1439.5, 1410.2, 1372.5, 1312.1, 1234, 1165.4, 1112.3, 1047.7, 892.7, 865.1, 814.9, 783, 696.7, 579.6. HRMS (ESI): m/z calcd for $C_8H_8NO_5$ $[M + H]^+$, 198.0402; found, 198.0406.

N9-Propyl-7-deazaadenine (^{7C}Ade). To a solution of 6-amino-7-deazapurine (1.00 g, 7.23 mmol) in anhydrous *N*,*N*-dimethylformamide (200 mL) was added NaH (0.10 g, 2.48 mmol) under argon. The reaction mixture was stirred for 30 min until H_2 evolution ceased. 1-Iodopropane (0.22 mL, 2.26 mmol) was then added, and the reaction mixture was stirred at room temperature for 24 h under argon. The solvent was removed under reduced pressure. The crude residue was dissolved in dichloromethane (200 mL) and washed with an aqueous solution of sodium hydrogen carbonate (10% m/m, 150 mL) and brine (150 mL). The organic layer was collected, dried over magnesium sulfate, filtered off, and concentrated in vacuo. The precipitate was recrystallized from dichloromethane to give the title compound in the form of a powder (0.70 g, 55% yield). ^{1}H NMR (300 MHz, DMSO-d_6): δ (ppm) 8.04 (s, 1H; *CH*), 7.13 (d, J = 3.4 Hz, 1H; *CH*), 6.87 (s, 2H; NH_2), 6.51 (d, J = 3.4 Hz, 1H; *CH*), 4.05 (t, J = 7.1 Hz, 2H; CH_2), 1.90−1.61 (m, 2H; CH_2), 0.81 (t, J = 7.4 Hz, 3H; CH_3). ^{13}C NMR (500 MHz, DMSO): δ (ppm) 157.84 (C6), 151.89 (C2), 150.01 (C4), 124.52 (C8), 102.77 (C5), 98.68 (C7), 45.76 (C10), 23.70 (C11), 11.54 (C12). IR (ν/cm^{-1}): 1680, 1639.6, 1612.6, 1568.2, 1502.7, 1467.9, 1415.8, 1363.8, 1334.8, 1305.9, 1215.2, 1084.1, 1047.4, 1022.3, 960.62, 925.9, 879.6, 792.8, 752.3, 733, 700, 673.2. HRMS (ESI): m/z calcd for $C_9H_{13}N_4$ $[M + H]^+$, 177.1140; found, 177.1113.

https://dx.doi.org/10.1021/acs.inorgchem.0c01210
Inorg. Chem. XXXX, XXX, XXX−XXX

*N9-Propyl-6-chloro-2-amino-7-deazapurine (**Cl-^{7C}Gua**).* 6-Chloro-2-amino-7-deazapurine (1.00 g, 5.90 mmol) was dissolved in anhydrous *N*,*N*-dimethylformamide (100 mL), and NaH (0.24 g, 6.00 mmol) was added under argon. The reaction mixture was stirred until H_2 evolution ceased. 1-Iodopropane (0.58 mL, 6.00 mmol) was then added, and the solution was stirred for 24 h at room temperature under argon. The solvent was removed under reduced pressure. The crude precipitate was dissolved in dichloromethane (200 mL) and washed with aqueous sodium hydrogen carbonate (10% m/m, 150 mL) and brine (150 mL). The organic layer was collected, dried over magnesium sulfate, filtered, and concentrated in vacuo. The sample was then recrystallized from dichloromethane to give the title compound in the form of a powder (0.85 g, 68% yield). ^{1}H NMR (300 MHz, DMSO-d_6): δ (ppm) 7.17 (d, J = 3.5 Hz, 1H; *CH*), 6.61 (s, 2H; NH_2), 6.28 (d, J = 3.4 Hz, 1H; *CH*), 3.97 (t, J = 7.1 Hz, 2H; CH_2), 1.73 (m, 2H; CH_2), 0.82 (t, J = 7.3 Hz; 3H; CH_3). HRMS (ESI): m/z calcd for $C_9H_{12}ClN_4$ $[M + H]^+$, 211.0750; found, 211.0732.

*N9-Propyl-7-deazaguanine (**^{7C}Gua**).* **Cl-^{7C}Gua** (0.40 g, 1.90 mmol) was refluxed in a hydrochloric acid (25 mL, 1 M) and ethanol (5 mL) mixture for 2 h. After the mixture was cooled to room temperature, the pH was adjusted to ca. 7 using sodium hydroxide and the suspension was cooled in an ice bath for 1 h. The precipitate was collected by filtration and dried in vacuo to afford the title compound in the form of crystals (0.05 g, 15% yield). ^{1}H NMR (300 MHz, DMSO-d_6): δ (ppm) 10.22 (s, 1H; *NH*), 6.71 (d, J = 3.2 Hz, 1H; *CH*), 6.19 (d, J = 3.3 Hz, 2H; NH_2), 6.17 (s, 1H; *CH*), 3.85 (t, J = 7.0 Hz, 2H; CH_2), 1.68 (m, 2H; CH_2), 0.82 (t, J = 7.3 Hz, 3H; CH_3). ^{13}C NMR (500 MHz, DMSO-d_6): δ (ppm) 159.1 (C6), 152.9 (C2), 150.5 (C4), 120.4 (C8), 101.4 (C7), 100.3 (C5), 45.81 (C10), 23.7 (C11), 11.5 (C12). IR (ν/cm^{-1}): 3402.7, 3173.1, 2874.1, 1660.8, 1608.7, 1539.3, 1508.4, 1433.2, 1410.1, 1369.6, 1334.8, 1304, 1213.3, 1180.5, 1072.5, 889.2, 850.7, 785.1, 717.8, 677.1, 601.8, 555.5. HRMS (ESI): m/z calcd for $C_9H_{13}N_4ONa$ $[M + H]^+$, 193.1089; found, 193.1086.

Synthesis of the Complexes. *[Cu(mcheld)(H_2O)$_2$] (**1Cu**).* To an aqueous solution of $Cu(CH_3COO)_2$ (0.09 g, 0.50 mmol) was added an aqueous solution of mcheld (0.10 g, 0.50 mmol) dropwise with stirring. The resulting solution was heated to 90 °C and left at this temperature with stirring for 30 min. A light blue precipitate appeared, which was filtered off and washed with water, ethanol, and ether. The filtrate was left to crystallize by slow evaporation from the aqueous solution. After a few days, blue single crystals suitable for X-ray diffraction were collected (0.07 g, 50% yield). Anal. Calcd for $C_8H_9CuNO_7$: C, 32.60; H, 3.08; N, 4.75. Found: C, 32.55; H, 3.75; N, 4.81.

*[Cu(mcheld)(N3-Cyt)(H_2O)]·3H_2O (**1Cu_Cyt**).* To a warm aqueous solution (15 mL) of 1-methylcytosine (0.09 g, 0.07 mmol) was added an aqueous solution (10 mL) of **1Cu** (0.02 g, 0.07 mmol) dropwise. The solution was heated to 65 °C and left at this temperature with stirring for 30 min. When the solution appeared clear, it was left to crystallize by slow solvent evaporation at room temperature. After a few days, blue single crystals suitable for X-ray diffraction were formed (0.01 g, 40% yield). Anal. Calcd for $C_{13}H_{14}CuN_4O_7{\cdot}3H_2O$: C, 34.25; H, 4.42; N, 12.29. Found: C, 34.55; H, 4.50; N, 12.54.

*[Cu(mcheld)(N7-Ade)(H_2O)]·2H_2O (**1Cu_Ade**).* To a warm aqueous solution (15 mL) of *N9*-ethyladenine (0.02 g, 0.10 mmol) was added an aqueous solution (15 mL) of **1Cu** (0.03 g, 0.10 mmol) dropwise. The solution was heated to 65 °C and left at this temperature with stirring for 30 min. The precipitate was collected by filtration and dried in vacuo to afford the title compound in the form of a powder (0.04 g, 87% yield). Anal. Calcd for $C_{15}H_{16}CuN_6O_6{\cdot}6.6H_2O$: C, 32.03; H, 5.30; N, 14.94. Found: C, 31.84; H, 4.93; N, 15.45. The precipitate was recrystallized by room-temperature slow evaporation in DMF, giving blue single crystals suitable for X-ray diffraction after a few days. The detection of higher water content by elemental analysis than by X-ray diffraction (*vide infra*) could be due to the presence of surface-absorbed moisture.

*[Cu(mcheld)(N7-Gua)(H_2O)] (**1Cu_Gua**).* To an aqueous solution (15 mL) of *N9*-propylguanine (0.02 g, 0.10 mmol) was added an aqueous solution (10 mL) of **1Cu** (0.03 g, 0.10 mmol) dropwise. The solution was heated to 65 °C and left at this temperature with stirring for 30 min. A very thin precipitate was formed and eliminated by filtration. The clear solution was then left to crystallize at room temperature by slow solvent evaporation. After a few days, blue single crystals suitable for X-ray diffraction were collected (0.02 g, 47% yield). Anal. Calcd for $C_{16}H_{18}CuN_6O_7(H_2O)$: C, 39.39; H, 4.13; N, 17.23. Found: C, 39.71; H, 4.22; N, 17.12. The detection of higher water content by elemental analysis than by X-ray diffraction (*vide infra*) could be due to the presence of surface-absorbed moisture.

*[Cu(mcheld)(N1-^{7C}Ade)(H_2O)$_2$]·H_2O (**1Cu_^{7C}Ade**).* To an aqueous solution (15 mL) of **1Cu** (0.02 g, 0.07 mmol) was added an aqueous solution (10 mL) of the ligand (0.01 g, 0.07 mmol) dropwise. The solution was heated to 60 °C and left at this temperature with stirring for 30 min. A thin precipitate was formed and eliminated by filtration. The clear solution was then left to crystallize at room temperature by slow solvent evaporation. After a few days, blue single crystals suitable for X-ray diffraction were recovered (0.01 g, 32% yield). Anal. Calcd for $C_{17}H_{19}CuN_5O_6(H_2O)$: C, 43.35; H, 4.49; N, 14.87. Found: C, 43.18; H, 4.92; N, 14.70.

Single-Crystal X-ray Diffraction Structure Determination. X-ray diffraction data for **1Cu_^{7C}Ade** were collected using a Bruker X8 Proteum diffractometer equipped with a Cu (λ = 1.54178 Å) sealed rotating anode X-ray tube, a Bruker AXS Smart 6000 CCD detector, and an Oxford Cryostream 700 plus cooling apparatus. X-ray diffraction data for **1Cu**, **1Cu_Ade**, and **1Cu_Gua** were collected on a Bruker D8 Venture diffractometer equipped with either a Cu (λ = 1.54178 Å) or a Mo (λ = 0.71073 Å) X-ray tube, a Bruker AXS Photon 100 detector, and a Kryoflex II cooling apparatus. For all four of the complexes, data reduction was performed with the software APEX3,[32] while data correction for absorption was carried out using the software SADABS.[33] X-ray diffraction data for **1Cu_Cyt** were collected using a Bruker SMART APEX I diffractometer equipped with a Mo (λ = 0.71073 Å) X-ray tube and a Kryoflex cooling apparatus. In this case, data reduction was performed with the software SAINT V6.36A, while data correction for absorption was carried out using SADABS.[33] The structures were solved by direct methods as implemented in SHELXS-97,[34] which allowed the location of most of the atoms of the asymmetric unit. All the remaining non-hydrogen atoms were located from difference Fourier maps calculated from successive full-matrix least-squares refinement cycles on F^2 using SHELXL-2018/3.[34] The electron densities around the propyl group in **1Cu_Gua** and **1Cu_^{7C}Ade** were ill-defined: the central carbon atom of the propyl group was found to be disordered into two positions. Isotropic thermal displacement parameters were refined for the three carbon atoms of the propyl group, and no hydrogen atoms were located on them. Anisotropic thermal displacement parameters were assigned to all the other non-hydrogen atoms. The hydrogen atoms were located at idealized positions using HFIX instructions and described with isotropic thermal displacement parameters fixed at 1.2 or 1.5 times those of the atom to which they were bound. The main crystallographic information and experimental and data treatment details are provided in Table S1 in the Supporting Information.

Computational Details. Theoretical models were built from scratch using the Avogadro software.[35] Sodium counterions or protons were added to the phosphate groups, thus resulting in neutral model systems. After a partial geometry optimization of these molecules, using semiempirical methods (PM3) within the ORCA 4.2.1 computational program,[36,37] a suitable geometry was obtained for further full optimization by quantum mechanics *ab initio* calculations using the HF-3c method.[38] The latter method includes the so-called MINIX basis set and a correction of the basis set superposition error (BSSE) by means of the geometrical counterpoise gCP correction algorithm,[39] as well as the atom-pairwise London dispersion energy from the D3 dispersion correction scheme with the Becke−Johnson damping scheme (D3BJ).[40−42] The solvent effect was included by the so-called "implicit solvent model". Thus, the solute was placed in a cavity of roughly molecular shape, and the solvent was described by a continuum that interacts with the charges on the cavity

https://dx.doi.org/10.1021/acs.inorgchem.0c01210
Inorg. Chem. XXXX, XXX, XXX−XXX

Scheme 1. Synthesis of the Model Nucleosides *N9*-Propyl-7-deazaadenine (^{7C}Ade) and *N9*-Propyl-7-deazaguanine (^{7C}Gua)[a]

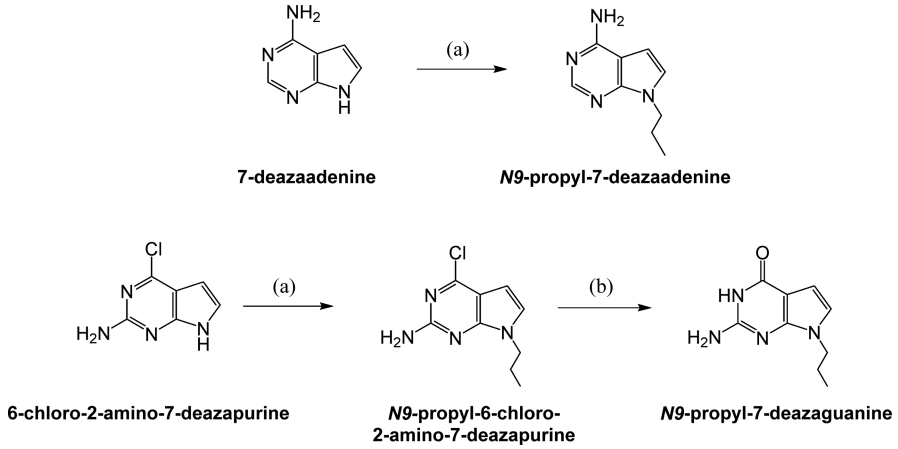

[a]Legend: (a) sodium hydride, 1-iodopropane, anhydrous *N*,*N*-dimethylformamide, rt, 24 h; (b) hydrochloric acid (1 M), reflux, 2 h.

surface. Specifically, the conductor-like polarizable continuum model (CPCM) was used for the computations of the DNA structure comprising only three base pairs ($\mathbf{DNA_3}$), using water as a solvent, which is an efficient way of accounting for solvent effects in quantum chemical calculations.[43] The solvent effect was not included for the calculations of larger $\mathbf{DNA_{15}}$ and $\mathbf{DNA_{10}}$ models, composed of 971 and 649 atoms, respectively, due to the extremely costly computational demand.

RESULTS AND DISCUSSION

Synthesis of 4-Methoxypyridine-2,6-dicarboxylic Acid (mcheld) and Model Nucleosides. The synthetic route to prepare 4-methoxypyridine-2,6-dicarboxylic acid (mcheld) consists of three steps (Scheme S1). The synthesis is initiated from the commercially available 4-hydroxypyridine-2,6-dicarboxylic acid, which is converted to diethyl-4-hydroxypyridine-2,6-carboxylate (decheld) in good yields, as described previously.[31] The successive reaction steps consist of the methylation of the hydroxyl functional group of decheld, using sodium hydride and iodomethane, to obtain diethyl 4-methoxypyridine-2,6-dicarboxylate (demcheld) in 94% yield. Finally, the demcheld ester is converted into the carboxylic acid mcheld using sodium hydroxide in water, affording it in 58% yield.

The model nucleosides *N9*-propyl-7-deazaadenine (^{7C}**Ade**) and *N9*-propyl-7-deazaguanine (^{7C}**Gua**) were prepared by following an adaptation of previous synthesis protocols (Scheme 1).[30,44] The synthesis of ^{7C}**Ade** was achieved in good yield via N-alkylation of the commercially available 7-deazaadenine using sodium hydride and 1-bromopropane, in anhydrous *N*,*N*-dimethylformamide. In the case of *N9*-propyl-7-deazaguanine (^{7C}**Gua**), the synthesis starts from 6-chloro-2-amino-7-deazapurine and the N9 position is blocked by introducing a propyl chain via N-alkylation, to form *N9*-propyl-6-chloro-2-amino-7-deazapurine. Then, a hydroxyl group displaces the chlorine atom by nucleophilic aromatic substitution in acidic conditions (1 M hydrochloric acid) to obtain ^{7C}**Gua**.

Synthesis and Crystal Structure of [Cu(mcheld)-(H_2O)$_2$] (1Cu). The reaction of copper(II) acetate and mcheld was carried out in water at 90 °C, leading to a light blue precipitate. The latter was recovered by filtration and recrystallized in water, isolating blue single crystals which were characterized by elemental analysis and single-crystal X-ray diffraction according to the formula [Cu(mcheld)(H_2O)$_2$] (**1Cu**).

1Cu crystallizes in the monoclinic space group $P2_1/n$ (Table S1). The asymmetric unit contains one copper(II) ion, one mcheld molecule, and two water molecules, all in general positions. The copper(II) ion is five-coordinated and adopts a distorted-square-pyramidal geometry ($\tau = 0.08$)[45] (Figure S1), as already observed in [Cu(Cheld)(H_2O)$_2$].[46] In **1Cu**, the mcheld ligand[56] shows the μ,κ^3-N_{10},O_2,O_4 coordination mode (Cu−N10 1.900(2) Å, Cu−O2 2.056(1) Å, Cu−O4 2.043(2) Å) and occupies three basal positions. Two water molecules complete the coordination sphere, occupying the basal position opposite to the pyrimidine nitrogen atom (Cu−O2w 1.939(2) Å) and the apical position (Cu−O1w 2.174(2) Å). The latter water molecule forms a slightly elongated Cu−O bond, in agreement with the Jahn−Teller distortion that typically occurs in five- or six-coordinated Cu(II) complexes.[47] Intermolecular hydrogen bonds[56] are present among neighboring [Cu(mcheld)(H_2O)$_2$] complexes, involving the carboxylic oxygen atoms of mcheld and the water molecules (O1w···O2w 2.925(2) Å, O1w···O3 2.706(2) Å, O1w···O5 2.698(2) Å, O2w···O2 2.693(2) Å, O2w···O4 2.973(2) Å, O2w···O5 2.712(2) Å) (Figure S2). Overall, these interactions bring about the formation of a 3D supramolecular network. The methylation of the hydroxyl group of mcheld avoids the formation of intermolecular hydrogen bonds via this position.[48,49] As shown below, this feature is important regarding the coordination of the [Cu(mcheld)] fragment to nucleobases and nucleosides, since it favors the formation of hydrogen bonds exclusively between the carboxylic groups of mcheld and the donor or acceptor groups of the nucleobase moiety.[55]

Synthesis and Crystal Structure of mcheld-Cu-Nucleoside Complexes. The interaction of **1Cu** with a number of model nucleobases (Scheme 2) was studied in the solid state and solution by means of single-crystal X-ray diffraction and CD spectroscopy, respectively.

The general procedure to obtain complexes of the type [Cu(mcheld)(model nucleoside)] consisted of adding a warm aqueous solution of **1Cu** to a warm solution of the appropriate model nucleobase and leaving the mixture to react at 65 °C for 30 min with stirring. The precipitate was then filtered off and left to crystallize by slow evaporation (in DMF or water; see

https://dx.doi.org/10.1021/acs.inorgchem.0c01210
Inorg. Chem. XXXX, XXX, XXX−XXX

Scheme 2. Model Nucleosides Employed in the Present Work[a]

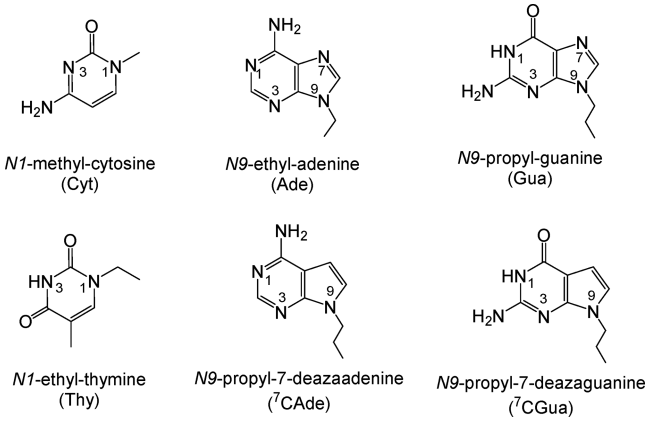

[a]For easy reading, the labels of the modified nucleobases avoid any reference to their alkyl functionalization.[57]

the Experimental Section). In all cases except for the Thy and ^{7C}**Gua** nucleobases, single crystals were formed after a few days and were characterized by X-ray diffraction as [Cu(mcheld)-(*N*3-Cyt)(H_2O)]·3H_2O (**1Cu_Cyt**), [Cu(mcheld)(*N*7-Ade)-(H_2O)$_2$]·2H_2O (**1Cu_Ade**), [Cu(mcheld)(*N*7-Gua)(H_2O)] (**1Cu_Gua**) and [Cu(mcheld)(*N1*-^{7C}Ade)(H_2O)]·H_2O (**1Cu_^{7C}Ade**).

The complex **1Cu_Cyt** crystallizes in the triclinic space group $P\bar{1}$ (Table S1). The asymmetric unit consists of one metal ion, one mcheld ligand, one Cyt nucleoside, and four water molecules, all in general positions. The copper(II) ion is six-coordinated and adopts a distorted-octahedral geometry. The mcheld ligand shows the μ,κ^3-N10,O2,O4 coordination mode (Figure 1-a) (Cu−N10 1.893(3) Å, Cu−O2 1.997(2) Å, Cu−O4 2.027(2) Å), occupying three equatorial positions, while the Cyt ligand shows the μ,κ^2-N3,O21 coordination mode (Figure 1a) (Cu−N3 1.956(3) Å, Cu−O21 2.711(3) Å), completing the equatorial plane with the pyrimidine nitrogen atom N3 and locating the ketonic oxygen atom O21, with a loose interaction, at one of the axial positions. One water molecule completes the coordination sphere (Cu−O1w 2.407(2) Å) at the remaining axial position, opposite to O21. Again, the longer axial Cu−O distances are reasonably the result of the Jahn−Teller effect. An intramolecular hydrogen bond is found between the coordinated water molecule O1w and the nitrogen atom N4 of the Cyt amino group (Figure 1a) (N4···O1w 2.822(2) Å). Intermolecular hydrogen bonds[56] are present between N4 and one non-coordinated water molecule (N4···O2w 2.863(4) Å) and among noncoordinated water molecules (O3w···O2w 2.821(5) Å, 2.826(3) Å, O3w···O3w 2.796(5) Å), as well as between water molecules and coordinated and dangling oxygen atoms of the carboxylate groups of mcheld (O4w···O2 2.886(4) Å, O4w···O4 2.866(4) Å, O1w···O5 2.775(4) and 2.841(4) Å). Overall, all the hydrogen-bond donor and acceptor atoms, from both mcheld and the Cyt moiety, are involved in hydrogen bonds (Figure 1b). The O1w···O5 interactions define a graph set motif of the type $R^2_4(8)$ (Figure S3).[50] In addition, each O2w···O3w···O3w···O2w segment (Figure 1b), running along the [001] crystallographic direction and lying on an inversion center, connects six [Cu(mcheld)(*N*3-Cyt)-(H_2O)] complexes. The crystal structure of **1Cu_Cyt** is

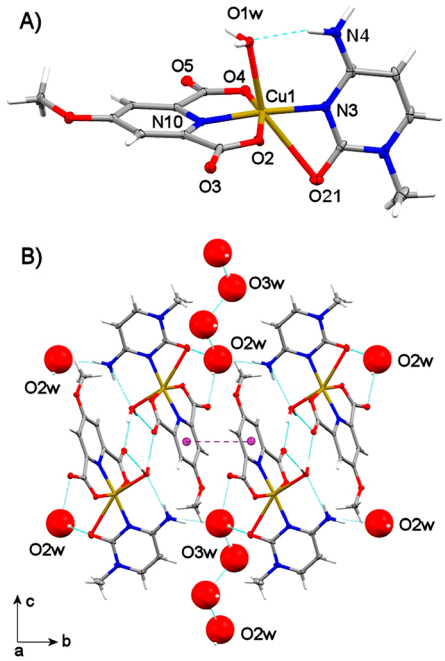

Figure 1. (a) Molecular structure of the complex [Cu(mcheld)(*N*3-Cyt)(H_2O)]·3H_2O (**1Cu_Cyt**) with thermal ellipsoids set at the 30% probability level. (b) Portion of the crystal structure of **1Cu_Cyt**, showing pairs of **1Cu_Cyt** complexes connected by hydrogen bonds (dashed cyan lines) and $\pi-\pi$ interactions (dashed purple line). The uncoordinated water molecules O4w (and the corresponding hydrogen bonds) have been omitted for clarity. The O2w and O3w noncoordinated water molecules have been represented as space-filling spheres.

further stabilized by the formation of $\pi-\pi$ interactions (distance between the centroids 3.596(2) Å, α = 0°, $\beta = \gamma$ = 27.25°) between the pyridine rings of mcheld (Figure 1b). The angle between the rms planes of Cyt and the [Cu(mcheld)] fragment is 77.64(11)°, highlighting the high deviation from coplanarity of the two ligands, likely enforced by the coordination of N3 and O21 to the same metal center.

The complex [Cu(mcheld)(*N*7-Ade)(H_2O)$_2$]·2H_2O (**1Cu_Ade**) crystallizes in the monoclinic space group $P2_1/n$ (Table S1). The asymmetric unit features one copper(II) ion, one mcheld ligand, one Ade nucleoside, and four water molecules, all in general positions. The copper(II) ion is six-coordinated in a distorted-octahedral geometry. The ligand mcheld shows the μ,κ^3-N10,O2,O4 coordination mode (Figure 2) (Cu−N10 1.953(4) Å, Cu−O2 2.229(3) Å, Cu−O4 2.310(4) Å), occupying three meridional positions within the octahedron. Ade is coordinated to the copper(II) ion through

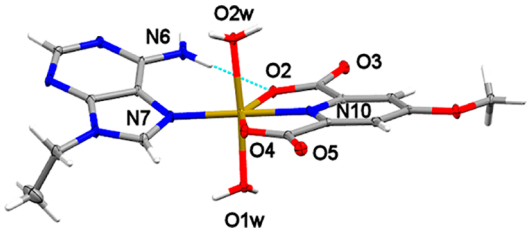

Figure 2. Molecular structure of the complex [Cu(mcheld)(*N*7-Ade)(H_2O)$_2$]·2H_2O (**1Cu_Ade**) with thermal ellipsoids set at the 30% probability level. The intramolecular hydrogen bond is depicted as a cyan dashed line.

https://dx.doi.org/10.1021/acs.inorgchem.0c01210
Inorg. Chem. XXXX, XXX, XXX−XXX

N7 (Cu−N7 1.960(4) Å), occupying the remaining meridional position. Two water molecules occupy the axial positions (Cu−O1w 2.032(3) Å, Cu−O2w 2.072(4) Å) (Figure 2). The observed *N7*-Ade coordination mode is reinforced by an intramolecular hydrogen bond, involving the Ade N6 exocyclic amino group as a donor and one carboxylate group of mcheld as an acceptor (N6···O2 2.846(6) Å) (Figure 2). This molecular recognition pattern has been previously observed in related aromatic amine analogues[27,51,52] and reasonably influences the low value of the angle between the rms planes of mcheld and the nucleobase (23.98(12)°).

The crystal structure is further stabilized by intermolecular hydrogen bonds[56] involving coordinated and uncoordinated water molecules, the aminic nitrogen atom N6 of Ade, and the carboxylate groups of mcheld (N6···O5 2.964(5) Å, O1w···O3 2.678(4) Å, O1w···O5 2.743(5) Å, O2w···O4w 2.749(4) Å, O2w···N3 2.819(6) Å, O3w···N1 2.834(5) Å, O3w···O4w 2.736(5) Å, O4w···O3 2.814(5) Å) (Figure 3). Interestingly,

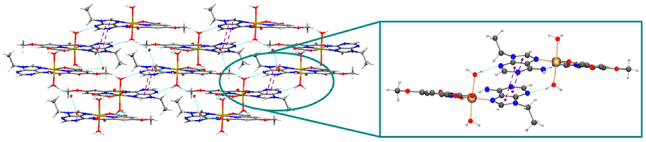

Figure 3. Portion of the crystal structure of **1Cu_Ade**. The hydrogen bonds (dashed cyan lines) involving the coordinated water molecules O2w lead to the formation of 1D double-strand motifs running along [001]. These motifs are connected by additional intermolecular $\pi-\pi$ interactions (purple lines), contributing to the formation of 2D supramolecular layers (a detail of the antiparallel $\pi-\pi$ interactions is provided in the inset).

upon consideration of the hydrogen bonds involving the coordinated water molecule O2w, a 1D double-strand motif running along the [001] direction can be envisaged (Figure 3). The strands interact through antiparallel $\pi-\pi$ stacking interactions between the five- and six-membered rings of Ade (distance between the centroids 3.552(3) Å, α = 2.30°, β = 19.93°, γ = 22.26°) (Figure 3 and Figure S4). Further hydrogen bond interactions define a 3D supramolecular network, in which two graphs set motifs of the kinds $R^3_4(10)$ and $R^3_2(10)$ can be identified (Figure S5).

The complex **1Cu_Gua** crystallizes in the monoclinic space group *Cc* (Table S1). The asymmetric unit consists of one copper(II) ion, one mcheld ligand, one Gua nucleoside, and one water molecule, all in general positions. The copper(II) ion adopts a distorted-square-pyramidal geometry (τ = 0.20)[45] (Figure 4). The mcheld ligand shows the μ,κ^3-N10,O2,O4 coordination mode (Cu−N10 1.908(4) Å, Cu−O2 2.061(4) Å, Cu−O4 2.046(4) Å), occupying three basal positions of the pyramid. The nucleobase Gua is coordinated to the copper(II) ion through N7 (Cu−N7 1.979(4) Å), occupying the fourth basal position. The apical position is occupied by a water molecule (Cu−O1w 2.155(4) Å). An intramolecular hydrogen bond is present between the water molecule and the keto group oxygen atom O61 of the nucleobase (Figure 4) (O1w···O61 2.698(5) Å). Moreover, intermolecular hydrogen bonds[56] are observed between the water molecule and the carboxylic atom O4 of mcheld (O1w···O4 2.746(6) Å), which leads to the formation of a 1D supramolecular chain of collinear metal ions 5.3 Å apart running along [010] (Figure S6). Hydrogen bonds are also present between the guanine N2 amino group and the carboxylate O5 atom of mcheld and between the

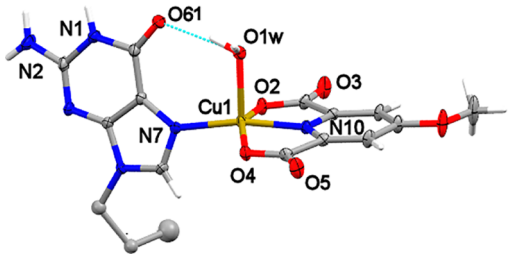

Figure 4. Molecular structure of [Cu(mcheld)(*N7*-Gua)(H_2O)] (**1Cu_Gua**) with thermal ellipsoids set at the 30% probability level. The intramolecular hydrogen bond interaction is highlighted by a cyan dashed line. For clarity, an ordered model has been adopted for the Gua propylic residue.

guanine endocyclic N1 nitrogen atom and the carboxylate O3 atom of mcheld (N2···O5 2.988(7) Å, N1···O3 2.827(7) Å) (Figure S7). Overall, a 3D network of intermolecular hydrogens bond is formed. The [Cu(mcheld)] fragment and the Gua moiety are not coplanar, with an angle between their rms planes of 78.94(10)°. This non-negligible deviation from planarity can be due to the repulsive interactions that take place between the Gua keto group and the mcheld carboxylate groups, which also allows for the formation of the intramolecular hydrogen bond. No $\pi-\pi$ stacking interactions are observed in the crystal structure.

The interaction of complex **1Cu** with Ade and Gua derivatives occurs via the Hoogsteen-position N7 atom, as is evidenced by the complexes **1Cu_Ade** and **1Cu_Gua**, respectively. This metal−nucleoside binding mode is expected, since the N7 position is usually preferred by metal ions that interact with purine nucleobases/nucleosides, especially guanine.[53] The fact that no interaction was observed via the Watson−Crick position (the N1 atom) prompted us to use a different strategy to evaluate this alternative binding mode that could also occur when Cheld-Cu complexes are introduced in a DNA molecule. Thus, 7-deazapurine analogues were employed, namely *N9*-propyl-7-deazaadenine (**^{7C}Ade**) and *N9*-propyl-7-deazaguanine (**^{7C}Gua**), and their interactions toward **1Cu** were evaluated. This strategy has been already proven to be successful to study the interactions of metal ions toward Watson−Crick positions.[11,12]

The complex **1Cu_^{7C}Ade** was obtained upon reaction of **1Cu** with **^{7C}Ade** in water. This complex crystallizes in the triclinic space group $P\bar{1}$ (Table S1). The asymmetric unit contains one copper(II) ion, one mcheld ligand, one **^{7C}Ade** nucleoside, and one water molecule, all in general positions. The copper(II) ion shows a distorted-square-pyramidal coordination (τ = 0.10)[45] (Figure 5). The mcheld ligand shows the μ,κ^3-N10,O2,O4 coordination mode (Cu−N10 1.922(3) Å, Cu−O4 2.128(2) Å, Cu−O2 2.038(2) Å), occupying three basal positions. In this case, the nucleoside **^{7C}Ade** is coordinated to the copper(II) ion through the Watson−Crick position N1, occupying the fourth basal position of the pyramid (Cu−N1 1.974(3) Å) (Figure 5). The apical position is occupied by a water molecule (Cu−O1w 2.210(2) Å) (Figure 5).

The mcheld ligand and the **^{7C}Ade** nucleoside are not coplanar, with an angle between their rms planes of 45.47(7)°, considerably larger than the angle observed when the [Cu(mcheld)] fragment binds via the Ade-N7 atom (vide supra). Intra- and intermolecular hydrogen bonds are present between the **^{7C}Ade**-N6 amino protons and the carboxylate O2

https://dx.doi.org/10.1021/acs.inorgchem.0c01210
Inorg. Chem. XXXX, XXX, XXX−XXX

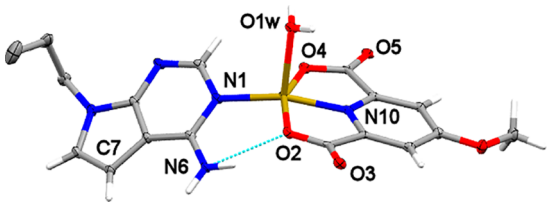

Figure 5. Molecular structure of the complex [Cu(mcheld)-(*N1*-^{7C}**Ade**)(H_2O)]·H_2O (**1Cu_^{7C}Ade**) with thermal ellipsoids set at the 30% probability level. The intramolecular hydrogen bond is highlighted by a dashed cyan line. The uncoordinated water molecule (and the corresponding hydrogen bonds) has been omitted for clarity. An ordered model has been adopted for the ^{7C}**Ade** propylic residue.

and O3 atoms of the mcheld ligand (N6···O2 2.768(4) Å and N6···O3 2.960(3) Å, respectively). Also, the water molecule O1w forms intermolecular hydrogen bonds[56] with the donor atoms of two different adjacent complexes (O1w···O4 2.790(4) Å, O1w···O5 2.717(3) Å, O2w···N3 2.956(4) Å), leading to a staircase-like 3D structure (Figure 6). No $\pi-\pi$ stacking interactions are present.

Interestingly, no complexes were either isolated or detected in solution when **1Cu** was reacted with thymidine and 7-deazaguanine derivatives (Scheme 2). This is probably due to the experimental conditions adopted. Unfortunately, although several attempts were performed at higher pH (9.5) to fully deprotonate such nucleosides, no complexes were isolated and further efforts still need to be done in this regard.

CD Spectroscopy Interaction Studies between Complex 1Cu and Single-Stranded DNA Homopolymers. The interaction of **1Cu** toward single-stranded DNA (ss-DNA) molecules was studied in an effort to evaluate the possible formation of a contiguous array of **1Cu_nucleobase** base pairs. To this aim, we used circular dichroism (CD) to unveil the interactions, at the oligomer level, between **1Cu** and different synthetic ss-DNA homopolymers containing the nucleoside analogues studied herein: namely, $d(Ade)_{15}$, $d(^{7C}Ade)_{15}$, $d(Cyt)_{15}$, and $d(Gua)_{10}$. The **1Cu** complex is CD inactive, and its UV–vis absorbance spectrum shows a broad band in the range 240–280 nm. Therefore, any induced circular dichroism (ICD) signal caused by the interaction of **1Cu** with the DNA homopolymers should be developed in this region. Unfortunately, in all cases, the addition of **1Cu** did not bring about significant changes in the CD spectra (Figure S8), thus indicating that the DNA helix conformation is not significantly altered. Therefore, nothing but weak interactions between **1Cu** and the ss-DNA homopolymers can be expected in solution. This is in contrast with the reported formation of individual mcheld-Cu-nucleobase base pair mismatches within double-stranded DNA scaffolds.[4] In that case, the copper(II) complex was covalently attached to the backbone of the DNA molecule and only one mismatch was introduced within the helix. On the other hand, in our study, the **1Cu** fragments are unrestricted in solution and the Cu···N(nucleoside) interaction does not seem to be strong enough to yield a Cu(II)-mediated base pair in solution. This fact, together with the hindering effect of several copper(II) ions close to each other, reasonably prevents the formation of stable Cu-ss-DNA hybrid systems in solution.

***Ab Initio* Computational Studies: Structural Features of 1Cu_nucleoside Pairs inside DNA Molecules.** As was mentioned above, the binding of complex **1Cu** toward canonical nucleosides has been previously reported in solution at the oligomer level in double-stranded DNA (except for thymidine),[4] while the crystal and molecular structures of the resulting **1Cu_nucleoside** monomers have been determined in this work. These results prompted us to evaluate the structural organization of **1Cu_nucleoside** pairs inside DNA double-helix structures and compare the structural features derived therefrom with those of the monomers described herein, as we believe that the DNA structure should have an important influence on the arrangement of these copper–base pairs. Furthermore, we aimed at evaluating the effect of Cu(II)-mediated nucleobase formation on the DNA structure that contains it.

The study of a DNA structure, in the solid state or solution, can be very difficult and expensive due to the difficulty in obtaining single crystals suitable for X-ray diffraction measurements or powdered batches in enough quantity to accomplish nuclear magnetic resonance studies (in the present case the latter studies are made even more difficult by the presence of the paramagnetic Cu(II) ions). More affordable spectroscopic or spectrometric studies (for instance, UV–vis absorption and fluorescence spectroscopy, CD, ESI-MS, MALDI-TOF) do not provide information on the three-dimensional structure. For this reason, theoretical computational studies can be a very important tool.

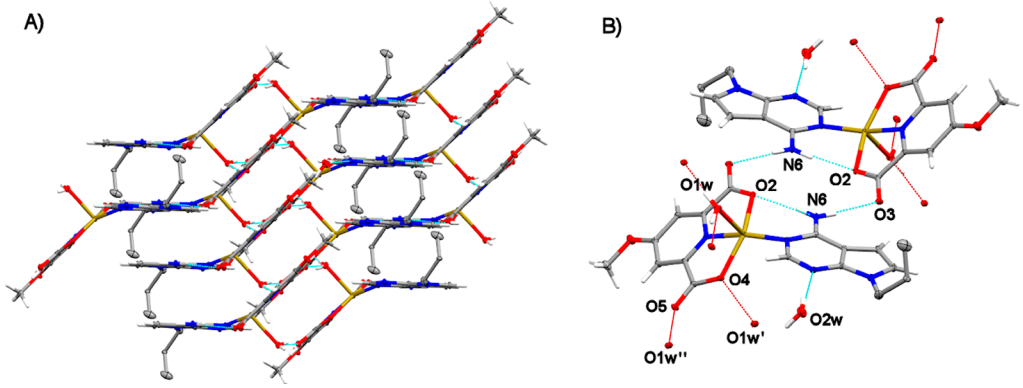

Figure 6. (A) In the crystal structure of **1Cu_^{7C}Ade**, hydrogen bonds (dashed cyan lines) involving the coordinated water molecule O1w and the exocyclic ^{7C}**Ade** amino group lead to the formation of staircase motifs. (B) Detail of the symmetry-related hydrogen bond interactions present in each "step" of the staircase. Red dotted lines represent hanging contacts.

https://dx.doi.org/10.1021/acs.inorgchem.0c01210
Inorg. Chem. XXXX, XXX, XXX–XXX

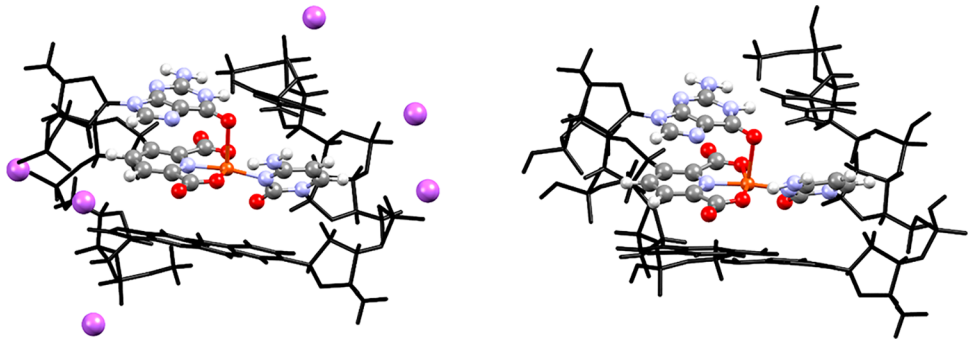

Figure 7. *Ab initio* HF-3c optimized geometries for the structures **DNA_3-Na** (left) and **DNA_3-H** (right) hosting the **1Cu_Cyt** complex.

Table 1. Comparison of the Relevant Bond Distances (Å) and Dihedral Angles (deg) of the 1Cu_Cyt Base Pair in the DNA_3 Optimized Models with the Experimental Values[a]

	exptl **1Cu_Cyt**	**DNA_3-Na**[b]	**DNA_3-H**[c]	**DNA_3-H-SE**[d]
Cu−N10	1.893	1.902 (0.009)	1.924 (0.031)	1.966 (0.073)
Cu−O2	1.997	1.900 (−0.097)	1.908 (−0.089)	1.923 (−0.074)
Cu−O4	2.027	1.900 (−0.127)	1.9 (−0.127)	1.916 (−0.111)
Cu−O_{axial}	2.407	2.527 (0.120)	2.504 (0.097)	2.488 (0.081)
Cu−N3	1.956	1.939 (−0.017)	1.965 (0.009)	1.977 (0.021)
Cu−O21	2.711	2.844 (0.133)	2.957 (0.246)	2.948 (0.237)
interplanar angle	77.7	47.6 (−30.1)	36.6 (−41.1)	34.9 (−42.8)
$C1'_{Gua}\cdots C1'_{Cyt}$		10.509	10.656	10.668
$C1'_{1Cu}\cdots C1'_{Cyt}$		8.759	9.284	9.566
$C1'_{Gua}\cdots C1'_{Cyt}$		10.760	10.682	10.688

[a]Deviations with respect to the latter are shown in parentheses. [b]Na indicates the use of sodium(I) as a cation. [c]H indicates the use of a proton as a cation. [d]SE indicates that the "solvent effect" has been included in the calculation.

We have employed computational calculations to study the structure of a 10-mer and a 15-mer DNA duplex model containing one Cu(II)-mediated base pair covalently attached to the DNA structure. Although they could be considered simple, these models enable us to study a realistic structure. Within the available theoretical models, molecular mechanics is not a valid method in the presence of metal ions such as Cu(II), while semiempirical models, although parametrized, can result in significant errors in the estimation of bond distances and angles.

Therefore, we strongly believe that the most useful methods to approach a DNA molecule of ca. 1000 atoms and containing metal ions are the *ab initio* and QMM methodologies. The latter approach, though faster, has the problem of validation. In our case, we do not have a reliable starting DNA structure to be validated. Thus, we decided not to use an approach that could lead to artifacts but rather to carry out a theoretical−computational structural study using the *ab initio* HF-3c method for DNA molecules holding the **1Cu_Cyt** or **1Cu_Gua** base pair located in the middle of the double helix. We have selected these Cu(II)−base pairs, as they exhibited the longest deviation from coplanarity between the [Cu(mcheld)] fragment and the Cyt or Gua bases in their crystal structure (see Synthesis and Crystal Structure of mcheld-Cu-Nucleoside Complexes), and thus they will potentially have a greater effect on the DNA double-helix conformation.

To this purpose, we have followed a bottom-up strategy, starting with the study of the **1Cu_Cyt** complex, followed by the study of a 3-mer DNA molecule containing the **1Cu_Cyt** base pair in the center of the structure, and finally performing calculations for 10-mer and 15-mer DNA molecules containing the **1Cu_Cyt** or **1Cu_Gua** complexes. To the best of our knowledge, this is the first time that a duplex DNA molecule containing metal-mediated base pairs has been studied at this computational level.

Single Model Complex. Initially, we carried out a theoretical study of the **1Cu_Cyt** molecular structure, starting from the experimentally determined one, to validate the theoretical *ab initio* HF-3c method employed in our following studies. After this preliminary study, we compared the computational results (**1Cu_Cyt-S**) with the experimental results, giving special attention to the interaction of the Cyt base with the copper(II) ion. Subsequently, we performed additional studies taking into account solvent effects (**1Cu_Cyt-SE**), using water as the solvent, and removing the coordinated water molecule (**1Cu_Cyt-NW**) to evaluate the consequence of the absence of the sixth coordination position observed experimentally.

For **1Cu_Cyt-S**, the results show a good agreement among the calculated and observed Cu−O and Cu−N distances (Table S2), with the greatest deviations observed for the Cu−O2 and Cu−O4 distances and for the angle between the [Cu(mcheld)] fragment and Cyt base (by 10°; see Figure S9). When the calculations were repeated with the solvent effects (**1Cu_Cyt-SE**) or without the coordinated water molecule (**1Cu_Cyt-NW**) taken into account, the results were very similar, and no significant differences were observed.

Model Systems of Three Base Pairs. After validating the theoretical model of **1Cu_Cyt** with the experimental observations, we set out to study how the scaffolding of a DNA molecule would affect the conformation of the **1Cu_Cyt** base pair. In an effort to work with the simplest DNA model, we studied a DNA duplex structure comprising only three base

https://dx.doi.org/10.1021/acs.inorgchem.0c01210
Inorg. Chem. XXXX, XXX, XXX−XXX

pairs (**DNA$_3$**), constructed with the sequences 5′-(G **1Cu** G)-3′ and 5′-(CCC)-3′. This **DNA$_3$** molecule represents a good starting point before studying larger DNA molecules (*vide infra*) because it takes into account the influence of the base pairs above and below the **1Cu_Cyt** base pair, which has been positioned in the middle.

For these calculations, the counteranions (namely the phosphate groups) were treated with either sodium cations (**DNA$_3$-Na**) or protons (**DNA$_3$-H**) and the results obtained with the two strategies were compared. We also evaluated the influence of the solvent effect on the latter model (**DNA$_3$-H-SE**).

In all cases, the copper(II) ion is five-coordinated in a square-pyramidal geometry. The mcheld ligand shows the μ,κ^3-N10,O2,O4 coordination mode, occupying three equatorial positions, while the Cyt ligand acts as a monodentate ligand via N3 coordination, completing the basal plane. Remarkably, the axial position of the copper(II) coordination sphere now involves a neighboring nucleotide, and the copper(II) ions bind the guanine-O6 atom (Figure 7). This situation is similar to that observed in the crystal structure of a related copper-mediated base pair in DNA.[20]

The results show that in all cases there is a good agreement among the experimental and calculated bond distances involving the copper(II) ions (Table 1). The greatest deviations are again observed for the Cu−O2 and Cu−O4 distances and the interplanar angle between the [Cu(mcheld)] fragment and the cytosine base. Both **DNA$_3$** models show a significantly lower interplanar angle in comparison to the complex alone, which can be explained as a result of the influence of the DNA scaffold: the presence of the base pairs above and below the **1Cu_Cyt** base pair reasonably limits the rotation around the Cu−N3 bond. In this regard, the best agreement was found with the **DNA$_3$-Na** model, which exhibits an interplanar angle closer to the observed angle.

The glyosidic C1′···C1′ distances between opposite nucleobases are within the range 10.5−10.8 Å observed for natural base pairs, while they are significantly smaller for the **1Cu_Cyt** base pair (<9.56 Å), especially in the **DNA$_3$-Na** model, which displays a distance of 8.76 Å.

Interestingly, the presence of the **1Cu_Cyt** complex seems to affect more the conformation of the strand that holds the **1Cu** metal fragment. This is highlighted by the shorter P···P distance (5.94 Å) of contiguous phosphate groups attached to the sugar unit of [Cu(mcheld)] vs the other P···P distances in the duplex (>6.39 Å). This is situation is more pronounced in the case of the **DNA$_3$-Na** model, where the phosphate groups are separated by only 4.2 Å and seem to be stabilized by two nearby sodium cations (Na···Na 3.766 Å) that bridge both phosphate groups (Na···O 2.068−2.132 Å) (Figure 8).

It is worth mentioning that, since a water molecule was found to be involved in the coordination sphere of copper(II) in the **1Cu_Cyt** complex, the **DNA$_3$-H** model was also studied in the presence of a water molecule placed near the metal ion. In this situation, the results also showed the formation of the Cu(II)−Gua(O6) bond (Figure S10).

Full DNA Model Systems. Finally, we performed a theoretical study for 15-mer (**DNA$_{15}$**) and 10-mer (**DNA$_{10}$**) duplexes containing the **1Cu_Cyt** and **1Cu_Gua** base pairs, respectively, in the middle of the double helixes. In an effort to reduce the influence of arbitrary DNA sequences surrounding the copper-mediated base pair, the model sequences have been designed to contain only guanosine and cytidine bases (Table 2).

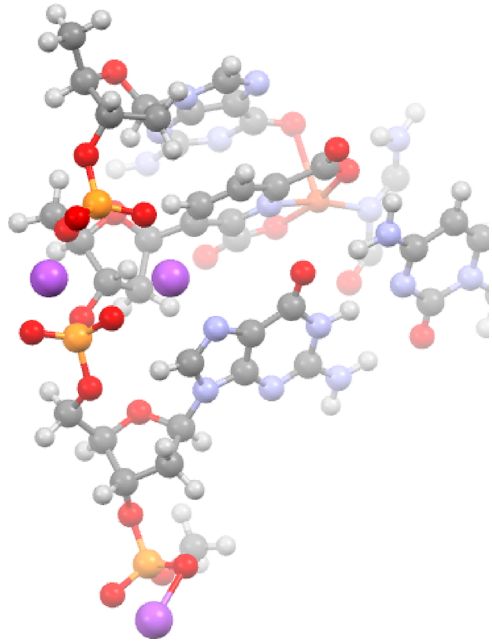

Figure 8. Close view of the HF-3c optimized geometry for **DNA$_3$-Na** showing the position of two sodium ions (purple) bridging contiguous phosphate groups.

Table 2. DNA Duplexes Employed in the *Ab Initio* Calculations

duplex	sequence
DNA$_{15}$	5′-(CCC CCC C **C** C CCC CCC)-3′
	3′-(GGG GGG G **1Cu** G GGG GGG)-5′
DNA$_{10}$	5′-(CCC C **1Cu** C CCC C)-3′
	3′-(GGG G **G** G GGG G)-5′

First, we studied the structure of the 15-mer duplex **DNA$_{15}$**, compensating the negative charge of the phosphate groups with the presence of sodium cations (**DNA$_{15}$-Na**). It is worth noting that this study required an extensive computational effort, as up to 28 sodium cations were considered in the *ab initio* calculations.

We also performed the same calculation using protons as counterions (**DNA$_{15}$-H**) to reduce the computational cost, and the results were compared to those obtained with **DNA$_{15}$-Na** to evaluate the consequences of this approach. Finally, we studied duplex **DNA$_{10}$** by treating the phosphate groups with protons (**DNA$_{10}$-H**). The solvent effect was not taken into account in any case, due to the great calculation effort that this would have required.

The optimized geometry of duplex **DNA$_{15}$-Na** contains 15 base pairs and completes an entire turn, holding a right-handed B-like conformation (Figure 9). The **1Cu_Cyt** base pair is placed at site 8, and copper(II) is six-coordinated and adopts a distorted-octahedral geometry, as seen for the **1Cu_Cyt** complex. The mcheld ligand shows the expected μ,κ^3-N10,O2,O4 coordination mode (Cu−N10 1.916 Å, Cu−O2 1.900 Å, Cu−O4 1.906 Å), occupying three basal positions. However, in contrast to the studied trimer **DNA$_3$-Na**, where the Cyt base acts as a monodentate ligand via N3 coordination, in duplex **DNA$_{15}$-Na** the Cyt base shows a μ,κ^2-N3,O21

https://dx.doi.org/10.1021/acs.inorgchem.0c01210
Inorg. Chem. XXXX, XXX, XXX−XXX

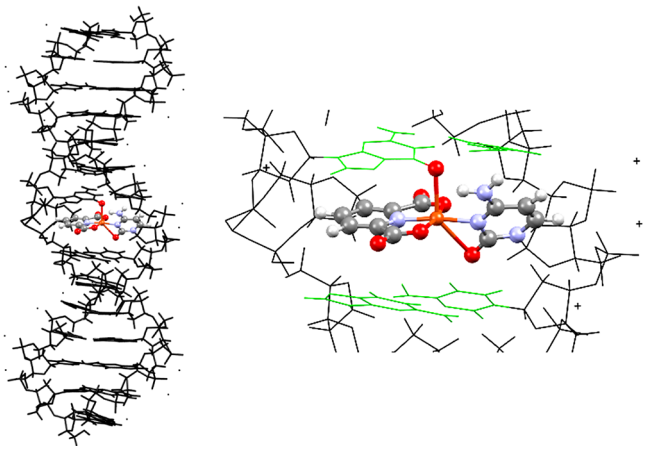

Figure 9. (left) The geometry-optimized duplex **DNA$_{15}$-Na**. (right) Closer view of the **1Cu_Cyt** base pair formed in the duplex structure showing the apical Cu−Gua-O6 and the Cu−Cyt-μ-N3,O21 bonds. Dots surrounding the double helix represent sodium cations which balance the negative charge of the phosphate DNA backbone. Color scheme: black, DNA structure different from the Cu(II)-mediated base pairs; green, neighboring nucleobases to **1Cu_Cyt** base pair.

coordination mode (Cu−N3 1.964, Cu−O21 2.703 Å), as seen in the X-ray crystal structure of the **1Cu_Cyt** complex (Table 3).

The axial position of the copper(II) coordination sphere involves a neighboring nucleotide: i.e., the copper(II) ion binds a neighboring Gua-O6 atom (Cu−O6 2.444 Å). It should be noted that this distance is considerably shorter than the sum of the Cu/O van der Waals radii. This situation has been also observed for the **DNA$_3$-Na** model, which displays a longer distance (2.527 Å), as well as for the crystal structure of the copper-mediated Dipic-Py base pair in DNA (Dipic = pyridine-2,6-dicarboxylate; Py = pyridine), although in that case the Cu−O6 distance was considerably longer (3.1 Å).[24] The fact that our *ab initio* calculation reveals the formation of the Cu−O axial bond with an adjacent guanidine nucleoside, for both **DNA$_3$-Na** and **DNA$_{15}$-Na** models, as reported for the DNA crystal structure, constitutes a validation that supports our theoretical method to study these copper-mediated base pairs in DNA duplexes.

Interestingly, the optimized geometry of **DNA$_{15}$-Na** reveals a larger interplanar angle (54.43°) between the [Cu(mcheld)] fragment and the cytidine base in comparison to that observed in the **DNA$_3$-Na** model (43.63°). This evidence shows that our original assumptions were not entirely correct; larger DNA molecules are not necessarily more constrained. Indeed, the rotation around the Cu−N3 bond inside the helix is allowed, leading to arrangements far from coplanarity. As a consequence, the Cu−O21 distance in our optimized **DNA$_{15}$-Na** model is very similar to that observed in **1Cu_Cyt**, indicating that this interaction could also occur in a duplex structure. This unexpected result indicates that the adjacent base pairs are not the only ones that influence the organization of the **1Cu_Cyt** base pair, but instead, the overall structure of a large DNA molecule has an effect. This could also be explained by the fact that the energy required to rotate the Cu−N3 bond and diminish the deviation from planarity of the complex can be dampened by a higher number of slight deviations from the optimal bond geometry of the higher number of bonds present in larger DNA structures.

In the duplex **DNA$_{15}$-Na**, the C1′···C1′ distances between opposite 2′-deoxyriboses of natural base pairs vary in the range 10.5−10.7 Å, which is consistent with a standard B-form conformation. However, as foreseen by our previous **DNA$_3$** models, at the copper−base pairs level (site 8) the C1′···C1′ distance is considerably shorter (8.3 Å), causing a narrowing of the double helix. The distortion caused by the **1Cu_Cyt** base pair in the duplex structure is analogous to what was observed for **DNA$_3$-Na**. Actually, two sodium(I) cations are also very close to each other (Na···Na 3.741 Å) and bridge two contiguous phosphate groups (Na···O 2.093−2.128 Å). In addition, stacking interactions occur between the mcheld ligand and the contiguous guanosine base to which the copper(II) ions coordinate through O6 coordination. The rest of the DNA structure presents a characteristic B-form conformation, without other remarkable changes. Therefore, the presence of **1Cu_Cyt** appears to only distort neighboring base pairs and is suitable to be formed in a DNA structure without major disruption of the structure.

The structure of **DNA$_{15}$-H** is shown in Figure 10. The optimized copper(II) ion is in a five-coordinated square-pyramidal geometry. The mcheld ligand shows the expected μ,κ^3-N10,O2,O4 coordination mode (Cu−N10 1.927 Å, Cu−O2 1.910 Å, Cu−O4 1.901 Å), occupying three basal positions. However, in contrast to the molecular structures of **1Cu_Cyt** and **DNA$_{15}$-Na**, where the Cyt ligand shows a μ,κ^2-N3,O21 coordination mode (*vide supra*), in duplex **DNA$_{15}$-H** the Cyt base acts as a monodentate ligand via N3 coordination,

Table 3. Comparison of the Relevant Bond Distances (Å) and Dihedral Angles (deg) in the Crystal Structures of the 1Cu_Cyt Base Pair and the DNA$_3$-Na, DNA$_{15}$-Na and DNA$_{15}$-H Optimized Models[a]

	exptl **1Cu_Cyt**	**DNA$_3$-Na**[b]	**DNA$_{15}$-Na**	**DNA$_{15}$-H**[c]
Cu−N10	1.893	1.902 (0.009)	1.916 (0.023)	1.927 (0.034)
Cu−O2	1.997	1.900 (−0.097)	1.900 (−0.097)	1.910 (−0.087)
Cu−O4	2.027	1.900 (−0.127)	1.906 (−0.121)	1.901 (−0.126)
Cu−O$_{axial}$	2.407	2.527 (0.120)	2.444 (0.037)	2.470 (0.063)
Cu−N3	1.956	1.939 (−0.017)	1.964 (0.008)	1.965 (0.009)
Cu−O21	2.711	2.844 (0.133)	2.703 (−0.008)	2.968 (0.257)
interplanar angle	77.7	47.6 (−30.1)	54.4 (−23.3)	38.9 (−38.9)
C1′$_{Gua}$···C1′$_{Cyt}$		10.509	10.547	10.681
C1′$_{1Cu}$···C1′$_{Cyt}$		8.759	8.347	9.263
C1′$_{Gua}$···C1′$_{Cyt}$		10.760	10.694	10.624

[a]Deviations with respect to the observed crystal structure are shown in parentheses. [b]Na indicates the use of sodium(I) as a cation. [c]H indicates the use of a proton as a cation.

https://dx.doi.org/10.1021/acs.inorgchem.0c01210
Inorg. Chem. XXXX, XXX, XXX−XXX

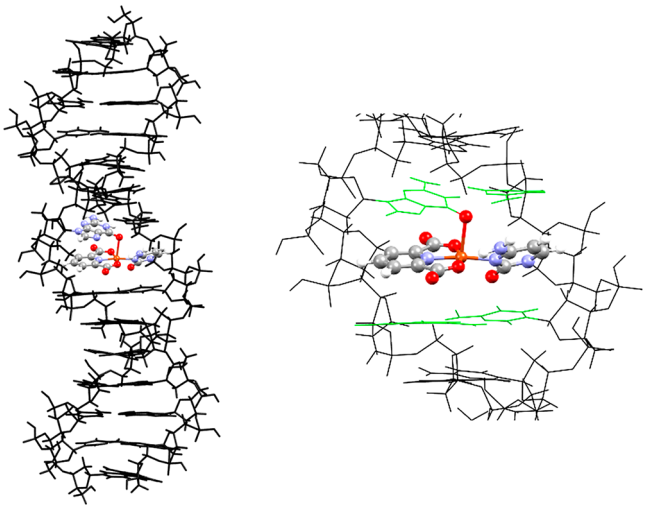

Figure 10. (left) The geometry-optimized duplex **DNA$_{15}$-H**. (right) Closer view of the **1Cu_Cyt** base pair formed in the duplex structure showing the Cu-Gua-O6 and Cu-Cyt-N3 bonds Color scheme: black, DNA structure different from the Cu(II)-mediated base pairs; green, neighboring nucleobases to **1Cu_Cyt** base pair.

completing the basal plane (Cu−N3 1.965 Å). This organization can be explained as a result of a smaller interplanar angle between the [Cu(mcheld)] fragment and the cytidine base (38.88°) and consequently a greater Cu−O21 distance (2.968 Å). The axial position of the copper(II) coordination sphere also involves a neighboring nucleotide: i.e., the copper(II) ion binds a neighboring Gua-O6 atom (Cu−O6 2.470 Å), as observed in **DNA$_{15}$-Na**. In this case, the C1′···C1′ distance between opposite 2′-deoxyriboses at the copper−base pairs level (site 8) is larger (9.2 Å), although the distance for natural base pairs remains within the expected 10.5−10.7 Å range. Importantly, the rest of the **DNA$_{15}$-H** structure does not show any major differences vs **DNA$_{15}$-Na**.

These results indicate that our *ab initio* calculations performed for the DNA molecules containing one **1Cu_Cyt** base pair can be successfully performed using sodium(I) ions or protons as counterions to compensate for the negative charge of the phosphate groups. The choice of one strategy or another will depend on the objective of the study. The **DNA$_{15}$-Na** model is more accurate by comparison with the observed molecular structure of **1Cu_Cyt**, at the expense of a considerably higher computational cost. Replacing Na^+ ions with protons (**DNA$_{15}$-H**) requires less demanding and more affordable computational resources. However, this model can lead to variations in the angles and bond distances of the **1Cu_Cyt** base pair, although the overall DNA structure is little affected. Therefore, these considerations must be taken into account depending on the aim of the calculation: namely, to study the overall DNA structure containing metal-mediated base pairs or to evaluate the arrangement of a specific base pair in the DNA structure. Although experimental structural data are required to evaluate the conformation in solution, namely high-resolution NMR data, our result indicates that the **1Cu-Cyt** base pair will exist inside the double helix with a large interplanar angle, as observed in the **DNA$_{15}$** models.

In an effort to assess the effect of the **1Cu_Gua** base pair in the DNA structure, we also performed a calculation using protons as counterions (**DNA$_{10}$-H**), as the computational cost was considerably lower (Figure S10). The **DNA$_{10}$-H** double helix contains 10 base pairs, holds a right-handed B-like form, and nearly completes a turn, with all the complementary cytidine and guanosine bases assembled via Watson−Crick hydrogen bonds along with stacking interactions. The [Cu(mcheld)] fragment is placed at site 5 (starting from the 5′-end), in the middle of the duplex, and binds guanosine 5 via the N7 atom, as observed in **1Cu_Gua** (*vide supra*). The copper(II) ion adopts a square-planar geometry, as previously described in related systems,[24] with no additional axial coordination observed. The mcheld ligand shows the expected μ,κ^3-N10,O2,O4 coordination mode, and the copper(II) ion is involved in shorter bonds (Cu−N10 1.925 Å, Cu−O2 1.884 Å, Cu−O4 1.903 Å) than in the crystal structure of **1Cu_Gua**. The guanosine moiety is coordinated to the copper(II) ion through N7 with a distance (Cu−N7 1.975 Å) very close to that present in the crystal structure. However, the spatial assembly of the units has considerably changed in comparison to the free **1Cu_Gua** monomer. In duplex **DNA$_{10}$-H**, the [Cu(mcheld)] fragment and the guanosine base self-assemble with a lower deviation from coplanarity, with an interplanar angle of 19.6°, instead of the 78.94(10)° angle observed in the crystal structure. Surprisingly, this arrangement appears to be possible despite the short distance observed between the guanosine keto group and the mcheld carboxylic atom (O61···O2 2.866 Å), which would be expected to generate a significant repulsion. This fact could be due to the strong influence that the overall duplex structure must have on the copper−base pair, indicating that the formation of the double helix may restrict the free rotation around the Cu−N7 bond, hampering the separation of the keto and carboxylic groups any further.

CONCLUSIONS

The formation of copper-mediated base pairs containing a pyridine-2,6-dicarboxylate derivative (mcheld) and model nucleosides (**Ade**, **Cyt**, **Gua**, and **^{7C}Ade**) was studied in the solid state and solution by means of single-crystal X-ray diffraction and CD spectroscopy, respectively. The former revealed the crystal and molecular structures of four mcheld-Cu-nucleoside systems, namely **1Cu_Cyt**, **1Cu_Ade**, **1Cu_^{7C}Ade**, and **1Cu_Gua**, which have been reported to occur individually in double-stranded DNA molecules.[4] Unfortunately, no single crystals suitable for X-ray diffraction could be isolated for the **1Cu_^{7C}Gua** compound. The versatility of these nucleoside analogues is evidenced in the case of adenine derivatives, where the coordination to the metal ion can be directed via either the Hoogsteen N7 position (as in **1Cu_Ade**), or the Watson−Crick N1 atom (as in **1Cu_^{7C}Ade**). Although the interaction metal−N1-Gua has not been observed in the present work, its formation cannot be ruled out; indeed, it is expected for the **1Cu_^{7C}Gua** complex and it has been previously reported for silver(I) ions.[54] The complex **1Cu_Cyt** demonstrates that the binding of **1Cu** could occur via both keto and amino groups simultaneously. The presence of a keto group in the nucleobase moiety induces a nearly perpendicular disposition of the [Cu(mcheld)] fragment vs the Gua or Cyt residues, as observed in **1Cu_Gua** and **1Cu_Cyt**, respectively, which could be attributed to the reciprocal repulsion of the keto and carboxylate groups. Interestingly, this high deviation from coplanarity between the [Cu(mcheld)] moiety and the nucleosides is not present in the **1Cu_Ade** and **1Cu_^{7C}Ade** derivatives, most likely due to the cooperation of the coordination bonds along with an

https://dx.doi.org/10.1021/acs.inorgchem.0c01210
Inorg. Chem. XXXX, XXX, XXX−XXX

intramolecular hydrogen bond interaction involving the exocyclic amino group NH_2. These results are in agreement with the stabilization trend observed for the Cheld-Cu-nucleobase system inside DNA duplexes (adenine > cytosine > guanine),[4] since a lower deviation from coplanarity of the units can facilitate the formation of intermolecular $\pi-\pi$ interactions and intramolecular hydrogen bonds between adenine and Cheld.

Importantly, the *ab initio* calculations performed for duplexes **DNA_{15}** and **DNA_{10}**, which embrace the **1Cu_Cyt** and **1Cu_Gua** base pairs in the middle of the duplexes, respectively, revealed that these base pairs can be formed inside DNA duplexes without significant distortion of the natural base pair arrangement. As a matter of fact, the geometry-optimized structures for duplexes **DNA_{15}** and **DNA_{10}** show that the **1Cu_nucleoside** base pairs remain in good harmony with the rest of the canonical Watson−Crick base pairs. The *ab initio* methodologies also revealed that the phosphate groups can be treated with Na^+ ions or protons, depending on the purposes of the computational calculations. A better agreement among the **1Cu_Cyt** calculated and experimental bond distances was found for the **DNA_{15}-Na** model, using Na^+ ions as counterions. However, the calculation performed on the **DNA_{15}-H** model, using protons as counterions, revealed some small deviations for the relevant bond distances at the Cu(II) ion, but the overall DNA structure can be correctly studied using this approach.

These results demonstrate that the organization of Cu−nucleobase base pairs can be studied in the solid state and in the context of a double helix using *ab initio* methodologies to evaluate the potential effects derived from the DNA scaffold, which may drive both metal coordination and the supramolecular assembly. These results can be extended to other metal-mediated base pairs.

■ ASSOCIATED CONTENT

Supporting Information

The Supporting Information is available free of charge at https://pubs.acs.org/doi/10.1021/acs.inorgchem.0c01210.

> Crystallographic information and relevant X-ray diffraction experimental details, additional figures of the crystal structures, circular dichroism spectra, additional figures for *ab initio* optimized geometries, and Cartesian coordinates (Å) for geometry-optimized molecules (PDF)

Accession Codes

CCDC 1835231−1835235 contain the supplementary crystallographic data for this paper. These data can be obtained free of charge via www.ccdc.cam.ac.uk/data_request/cif, or by emailing data_request@ccdc.cam.ac.uk, or by contacting The Cambridge Crystallographic Data Centre, 12 Union Road, Cambridge CB2 1EZ, UK; fax: +44 1223 336033.

■ AUTHOR INFORMATION

Corresponding Author

Miguel A. Galindo − *Departamento de Química Inorgánica, Universidad de Granada, 18071 Granada, Spain;* orcid.org/0000-0003-4355-4313; Email: magalindo@ugr.es

Authors

Alicia Dominguez-Martin − *Departamento de Química Inorgánica, Universidad de Granada, 18071 Granada, Spain;* orcid.org/0000-0001-8669-6712

Simona Galli − *Dipartimento di Scienza e Alta Tecnologia, Università dell'Insubria, 22100 Como, Italy;* orcid.org/0000-0003-0335-5707

José A. Dobado − *Grupo de Modelización y Diseño Molecular, Departamento de Química Orgánica, Universidad de Granada, 18071 Granada, Spain*

Noelia Santamaría-Díaz − *Departamento de Química Inorgánica, Universidad de Granada, 18071 Granada, Spain*

Antonio Pérez-Romero − *Departamento de Química Inorgánica, Universidad de Granada, 18071 Granada, Spain*

Complete contact information is available at: https://pubs.acs.org/10.1021/acs.inorgchem.0c01210

Author Contributions

The manuscript was written through contributions of all authors. All authors have given approval.

Notes

The authors declare no competing financial interest.

■ ACKNOWLEDGMENTS

Financial support from the Spanish MINECO (CTQ2017-89311-P), FEDER/Junta de Andalucía-Consejería de Economía y Conocimiento/Proyecto (A-FQM-465-UGR18), Junta de Andalucía (FQM-2293, FQM-283, FQM-174), and Unidad de Excelencia de Química aplicada a Biomedicina y Medioambiente (UGR) are acknowledged. S.G. acknowledges Università dell'Insubria for partial funding. We also thank the "Centro de Servicios de Informática y Redes de Comunicaciones" (CSIRC) (UGRGrid), University of Granada, for providing computing time.

■ REFERENCES

(1) Jones, M. R.; Seeman, N. C.; Mirkin, C. A. Programmable Materials and the Nature of the DNA Bond. *Science* **2015**, *347*, 1260901.

(2) Rothemund, P. W. K. Folding DNA to Create Nanoscale Shapes and Patterns. *Nature* **2006**, *440*, 297−302.

(3) Wilner, O. I.; Willner, I. Functionalized DNA Nanostructures. *Chem. Rev.* **2012**, *112*, 2528−2556.

(4) Meggers, E.; Holland, P. L.; Tolman, W. B.; Romesberg, F. E.; Schultz, P. G. A Novel Copper-Mediated DNA Base Pair. *J. Am. Chem. Soc.* **2000**, *122*, 10714−10715.

(5) Jash, B.; Müller, J. Metal-Mediated Base Pairs: From Characterization to Application. *Chem. - Eur. J.* **2017**, *23*, 17166−17178.

(6) Tanaka, K.; Shionoya, M. Synthesis of a Novel Nucleoside for Alternative DNA Base Pairing through Metal Complexation. *J. Org. Chem.* **1999**, *64*, 5002−5003.

(7) Takezawa, Y.; Shionoya, M. Metal-Mediated DNA Base Pairing: Alternatives to Hydrogen-Bonded Watson−Crick Base Pairs. *Acc. Chem. Res.* **2012**, *45*, 2066−2076.

(8) Takezawa, Y.; Müller, J.; Shionoya, M. Artificial DNA Base Pairing Mediated by Diverse Metal Ions. *Chem. Lett.* **2017**, *46*, 622−633.

(9) Polonius, F.-A.; Müller, J. An Artificial Base Pair, Mediated by Hydrogen Bonding and Metal-Ion Binding. *Angew. Chem., Int. Ed.* **2007**, *46*, 5602−5604.

(10) Megger, D. A.; Fonseca-Guerra, C.; Hoffmann, J.; Brutschy, B.; Bickelhaupt, F. M.; Müller, J. Contiguous Metal-Mediated Base Pairs Comprising Two Ag(I) Ions. *Chem. - Eur. J.* **2011**, *17*, 6533−6544.

(11) Santamaría-Díaz, N.; Méndez-Arriaga, J. M.; Salas, J. M.; Galindo, M. A. Highly Stable Double-Stranded DNA Containing

https://dx.doi.org/10.1021/acs.inorgchem.0c01210
Inorg. Chem. XXXX, XXX, XXX−XXX

Sequential Silver(I)-Mediated 7-Deazaadenine/Thymine Watson-Crick Base Pairs. *Angew. Chem., Int. Ed.* **2016**, *55*, 6170−6174.
(12) Méndez-Arriaga, J. M.; Maldonado, C. R.; Dobado, J. A.; Galindo, M. A. Silver(I)-Mediated Base Pairs in DNA Sequences Containing 7-Deazaguanine/Cytosine: Towards DNA with Entirely Metallated Watson-Crick Base Pairs. *Chem. - Eur. J.* **2018**, *24*, 4583−4589.
(13) Toomey, E.; Xu, J.; Vecchioni, S.; Rothschild, L.; Wind, S.; Fernandes, G. E. Comparison of Canonical versus Silver(I)-Mediated Base-Pairing on Single Molecule Conductance in Polycytosine DsDNA. *J. Phys. Chem. C* **2016**, *120*, 7804−7809.
(14) Jash, B.; Scharf, P.; Sandmann, N.; Fonseca Guerra, C.; Megger, D. A.; Müller, J. A Metal-Mediated Base Pair That Discriminates between the Canonical Pyrimidine Nucleobases. *Chem. Sci.* **2017**, *8*, 1337−1343.
(15) Al-Mahamad, L. L. G.; El-Zubir, O.; Smith, D. G.; Horrocks, B. R.; Houlton, A. A Coordination Polymer for the Site-Specific Integration of Semiconducting Sequences into DNA-Based Materials. *Nat. Commun.* **2017**, *8*, 720.
(16) Liu, S.; Clever, G. H.; Takezawa, Y.; Kaneko, M.; Tanaka, K.; Guo, X.; Shionoya, M. Direct Conductance Measurement of Individual Metallo-DNA Duplexes within Single-Molecule Break Junctions. *Angew. Chem., Int. Ed.* **2011**, *50*, 8886−8890.
(17) Xu, E.; Lv, Y.; Liu, J.; Gu, X.; Zhang, S. An Electrochemical Study Based on Thymine-Hg-Thymine DNA Base Pair Mediated Charge Transfer Processes. *RSC Adv.* **2015**, *5*, 49819−49823.
(18) Müller, J. Nucleic Acid Duplexes with Metal-Mediated Base Pairs and Their Structures. *Coord. Chem. Rev.* **2019**, *393*, 37−47.
(19) Fortino, M.; Marino, T.; Russo, N. Theoretical Study of Silver-Ion-Mediated Base Pairs: The Case of C-Ag-C and C-Ag-A Systems. *J. Phys. Chem. A* **2015**, *119*, 5153−5157.
(20) Li, G.; Liu, H.; Chen, X.; Zhang, L.; Bu, Y. Multi-Copper-Mediated DNA Base Pairs Acting as Suitable Building Blocks for the DNA-Based Nanowires. *J. Phys. Chem. C* **2011**, *115*, 2855−2864.
(21) Swasey, S. M.; Rosu, F.; Copp, S. M.; Gabelica, V.; Gwinn, E. G. Parallel Guanine Duplex and Cytosine Duplex DNA with Uninterrupted Spines of Ag I -Mediated Base Pairs. *J. Phys. Chem. Lett.* **2018**, *9*, 6605−6610.
(22) Schönrath, I.; Tsvetkov, V. B.; Zatsepin, T. S.; Aralov, A. V.; Müller, J. Silver(I)-Mediated Base Pairing in Parallel-Stranded DNA Involving the Luminescent Cytosine Analog 1,3-Diaza-2-Oxophenoxazine. *JBIC, J. Biol. Inorg. Chem.* **2019**, *24*, 693−702.
(23) Zimmermann, N.; Meggers, E.; Schultz, P. G. A Second-Generation Copper(II)-Mediated Metallo-DNA-Base Pair. *Bioorg. Chem.* **2004**, *32*, 13−25.
(24) Atwell, S.; Meggers, E.; Spraggon, G.; Schultz, P. G. Structure of a Copper-Mediated Base Pair in DNA. *J. Am. Chem. Soc.* **2001**, *123*, 12364−12367.
(25) Ghosh, S. K.; Ribas, J.; Bharadwaj, P. K. Metal-Organic Framework Structures of Cu(II) with Pyridine-2,6- Dicarboxylate and Different Spacers: Identification of a Metal Bound Acyclic Water Tetramer. *CrystEngComm* **2004**, *6*, 250−256.
(26) Das, B.; Baruah, J. B. Assembling of Copper(II) Dipicolinate Complexes. *Polyhedron* **2012**, *31*, 361−367.
(27) Del Pilar Brandi-Blanco, M.; Choquesillo-Lazarte, D.; Domínguez-Martín, A.; Matilla-Hernández, A.; González-Pérez, J. M.; Castiñeiras, A.; Niclós-Gutiérrez, J. Molecular Recognition Modes between Adenine or Adeniniun(1+) Ion and Binary M^{II}(Pdc) Chelates (M = Co-Zn; Pdc = Pyridine-2,6-Dicarboxylate(2-) Ion). *J. Inorg. Biochem.* **2013**, *127*, 211−219.
(28) Domínguez-Martín, A.; Choquesillo-Lazarte, D.; Dobado, J. A.; Vidal, I.; Lezama, L.; González-Pérez, J. M.; Castiñeiras, A.; Niclós-Gutiérrez, J. From 7-Azaindole to Adenine: Molecular Recognition Aspects on Mixed-Ligand Cu(II) Complexes with Deaza-Adenine Ligands. *Dalt. Trans.* **2013**, *42*, 6119−6130.
(29) Greco, E.; Aliev, A. E.; Lafitte, V. G. H.; Bala, K.; Duncan, D.; Pilon, L.; Golding, P.; Hailes, H. C. Cytosine Modules in Quadruple Hydrogen Bonded Arrays. *New J. Chem.* **2010**, *34*, 2634−2642.
(30) Nowick, J. S.; Chen, J. S.; Noronha, G. Molecular Recognition in Micelles: The Roles of Hydrogen Bonding and Hydrophobicity in Adenine-Thymine Base-Pairing in SDS Micelles. *J. Am. Chem. Soc.* **1993**, *115*, 7636−7644.
(31) Vermonden, T.; Branowska, D.; Marcelis, A. T. M.; Sudhölter, E. J. R. Synthesis of 4-Functionalized Terdendate Pyridine-Based Ligands. *Tetrahedron* **2003**, *59*, 5039−5045.
(32) *APEX3 Software,V2016.1*; Bruker AXS: Madison, WI, USA, 2016.
(33) Sheldrick, G. M. *SADABS 2016/2, Program for Empirical Absorption Correction of Area Detector Data*; University of Göttingen: Göttingen, Germany. 2016.
(34) Sheldrick, G. M. A Short History of SHELX. *Acta Crystallogr., Sect. A: Found. Crystallogr.* **2008**, *A64*, 112−122.
(35) (a) Hanwell, M. D.; Curtis, D. E.; Lonie, D. C.; Vandermeerschd, T.; Zurek, E.; Hutchison, G. R. Avogadro: An Advanced Semantic Chemical Editor, Visualization, and Analysis Platform. *J. Cheminf.* **2012**, *4*, 17. (b) *Avogadro: an open-source molecular builder and visualization tool. Version 1.XX*; http://avogadro.cc/.
(36) Neese, F. The ORCA Program System. *Wiley Interdiscip. Rev.: Comput. Mol. Sci.* **2012**, *2*, 73−78.
(37) Neese, F. Software Update: The ORCA Program System, Version 4.0. *Wiley Interdiscip. Rev.: Comput. Mol. Sci.* **2018**, *8*, e1327.
(38) Sure, R.; Grimme, S. Corrected Small Basis Set Hartree-Fock Method for Large Systems. *J. Comput. Chem.* **2013**, *34*, 1672−1685.
(39) Kruse, H.; Grimme, S. A Geometrical Correction for the Inter- and Intra-Molecular Basis Set Superposition Error in Hartree-Fock and Density Functional Theory Calculations for Large Systems. *J. Chem. Phys.* **2012**, *136*, 154101.
(40) Becke, A. D.; Johnson, E. R. A Density-Functional Model of the Dispersion Interaction. *J. Chem. Phys.* **2005**, *123*, 154101.
(41) Johnson, E. R.; Becke, A. D. A Post-Hartree−Fock Model of Intermolecular Interactions. *J. Chem. Phys.* **2005**, *123*, 024101.
(42) Johnson, E. R.; Becke, A. D. A Post-Hartree-Fock Model of Intermolecular Interactions: Inclusion of Higher-Order Corrections. *J. Chem. Phys.* **2006**, *124*, 174104.
(43) (a) Marenich, A. V.; Cramer, C. J.; Truhlar, D. G. Universal Solvation Model Based on Solute Electron Density and on a Continuum Model of the Solvent Defined by the Bulk Dielectric Constant and Atomic Surface Tensions. *J. Phys. Chem. B* **2009**, *113*, 6378−6396. (b) Tomasi, J.; Benedetta, M.; Cammi, R. Quatum Mechanical Continuum Solvation Models. *Chem. Rev.* **2005**, *105* (8), 2999−3094.
(44) Harnden, M. R.; Jarvest, R. L.; Bacon, T. H.; Boyd, M. R. Synthesis and Antiviral Activity of 9-[4-Hydroxy-3-(Hydroxymethyl)-but-l-Yl]Purines. *J. Med. Chem.* **1987**, *30*, 1636−1642.
(45) Addison, A. W.; Rao, T. N.; Reedijk, J.; Van Rijn, J.; Verschoor, G. C. Synthesis, Structure, and Spectroscopic Properties of Copper-(II) Compounds Containing Nitrogen-Sulphur Donor Ligands; the Crystal and Molecular Structure of Aqua[l,7-Bis(N-Methylbenzimidazol-2′-Yl)- 2,6-Dithiaheptane]Copper(II) Perchlorate. *J. Chem. Soc., Dalton Trans.* **1984**, *7*, 1349−1356.
(46) Hong-Ling, G.; Jian-Zhong, C. Hydrothermal Synthesis and Crystal Structures of Complex [Cu(CAM)(H_2O)$_2$]. *Chin. J. Inorg. Chem.* **2007**, *23*, 1072−1074.
(47) Janes, R.; Moore, E. A.; *Open University. Metal-Ligand Bonding*; Royal Society of Chemistry: London, 2004; pp 21−27.
(48) Mirzaei, M.; Eshtiagh-Hosseini, H.; Karrabi, Z.; Notash, B.; Bauzá, A.; Frontera, A.; Habibi, M.; Ardalani, M.; Shamsipur, M. Synthesis, Structure, Solution and DFT Studies of a Pyrazine-Bridged Binuclear Cu(II) Complex: On the Importance of Noncovalent Interactions in the Formation of Crystalline Network. *J. Mol. Struct.* **2015**, *1079*, 78−86.
(49) Vural, H.; Uçar, İ. A Mixed Experimental and Theoretical Study on Chelidamate Copper(II) Complex with 4-Methylpyrimidine. *J. Coord. Chem.* **2016**, *69*, 3010−3020.

https://dx.doi.org/10.1021/acs.inorgchem.0c01210
Inorg. Chem. XXXX, XXX, XXX−XXX

(50) Grell, J.; Bernstein, J.; Tinhofer, G. Graph-Set Analysis of Hydrogen-Bond Patterns: Some Mathematical Concepts. *Acta Crystallogr., Sect. B: Struct. Sci.* **1999**, *B55*, 1030−1043.
(51) Yenikaya, C.; Büyükkidan, N.; Sari, M.; Keşli, R.; Ilkimen, H.; Bülbül, M.; Büyükgüngör, O. Synthesis, Characterization, and Biological Evaluation of Cu(II) Complexes with the Proton Transfer Salt of 2,6-Pyridinedicarboxylic Acid and 2-Amino-4-Methylpyridine. *J. Coord. Chem.* **2011**, *64*, 3353−3365.
(52) Yenikaya, C.; Poyraz, M.; Sarı, M.; Demirci, F.; İlkimen, H.; Büyükgüngör, O. Synthesis, Characterization and Biological Evaluation of a Novel Cu(II) Complex with the Mixed Ligands 2,6-Pyridinedicarboxylic Acid and 2-Aminopyridine. *Polyhedron* **2009**, *28*, 3526−3532.
(53) Lippert, B. Multiplicity of Metal Ion Binding Patterns to Nucleobases. *Coord. Chem. Rev.* **2000**, *200−202*, 487−516.
(54) Kondo, J.; Tada, Y.; Dairaku, T.; Hattori, Y.; Saneyoshi, H.; Ono, A.; Tanaka, Y. A Metallo-DNA Nanowire with Uninterrupted One-Dimensional Silver Array. *Nat. Chem.* **2017**, *9*, 956−960.
(55) For the sake of comprehension, mcheld numbering in **1Cu** follows that adopted in the mcheld-Cu-nucleobase base pairs.
(56) Hydrogen bonds with D···A distances larger than 3.0 Å have been omitted. The reader is referred to the CIF file.
(57) The difference in the length of the alkyl chain is merely due to the access to specific starting materials at the time of the synthesis.

https://dx.doi.org/10.1021/acs.inorgchem.0c01210
Inorg. Chem. XXXX, XXX, XXX−XXX